Research Article

BIOMEDICAL Journal of Scientific & Technical Research

ISSN: 2574 -1241

DOI: 10.26717/BJSTR.2025.63.009837

Functionalized ZSM-5 via Combination Modification: Superhydrophobicity-Driven VOCs Capture and DFT-Elucidated Electron Transfer

Jiali Zhang[1,2]*, Xiaoyan Chen[1], Xue Li[1], Can Zhu[1,2], Qi Sun[1,2] and Yulong Zhang[1,2]*

[1]*College of Chemistry and Chemical Engineering, Henan Polytechnic University, PR China*

[2]*Henan Key Laboratory of Coal Green Conversion, Henan Polytechnic University, PR China*

***Corresponding author:** Yulong Zhang and Jiali Zhang, College of Chemistry and Chemical Engineering, Henan Polytechnic University, Jiaozuo, Henan 454000, PR China. Henan Key Laboratory of Coal Green Conversion, Henan Polytechnic University, Jiaozuo, Henan 454000, PR China

ARTICLE INFO

Received: August 09, 2025

Published: August 25, 2025

Citation: Jiali Zhang, Xiaoyan Chen, Xue Li, Can Zhu, Qi Sun and Yulong Zhang. Functionalized ZSM-5 via Combination Modification: Superhydrophobicity-Driven VOCs Capture and DFT-Elucidated Electron Transfer. Biomed J Sci & Tech Res 63(1)-2025. BJSTR. MS.ID.009837.

ABSTRACT

The emission of volatile organic compounds (VOCs) poses significant risks to public health and environmental safety. Adsorption has been recognized as a highly efficient technique for VOC abatement. However, the practical application of pristine ZSM-5 molecular sieves in VOC adsorption is substantially constrained by their inherent hydrophilic nature, which results in limited adsorption capacity. In this paper, ZSM-5 molecular sieve was modified by combination modification methods and evaluated by competitive adsorption breakthrough test. The modifications were monitored by XRD, SEM, FTIR, BET and ICP. Compared with the raw ZSM-5 molecular sieve, the engineered ZSM-5 demonstrated exceptional superhydrophobic characteristics, exhibiting an 80.7% reduction in water vapor adsorption capacity (decreasing from 7.87% to 1.52%). Concurrently, its toluene adsorption capacity exhibited a remarkable 438.9% enhancement, increasing from 1.87% to 10.24% under identical operational conditions. More importantly, the hydrophobicity, specific surface area, pore size and pore distribution were the critical factors affecting the VOCs adsorption of the ZSM-5 molecular sieve. Besides, DFT calculations were also performed to unveil the interaction mechanism of VOCs adsorption onto the surface of ZSM-5.

Keywords: ZSM-5; Superhydrophobic Structure; VOCs Adsorption; Toluene; DFT

Abbreviations: VOCs: Volatile Organic Compounds; PBE: Perdew–Burke–Ernzerhof; HOMO: Highest Occupied Molecular Orbital; LUMO: Lowest Unoccupied Molecular Orbital; TMCS: Trimethyl Chlorosilane

Introduction

Volatile organic compounds (VOCs) as a class of carbon-based organic chemicals can easily evaporate under the environmental conditions, which are discharged into the environment from various industrial, commercial and domestic practices [1-3]. As the major pollutants in the air, VOCs are responsible for the atmospheric photochemical reaction, photochemical smog and stratospheric ozone depletion etc [4,5]. Even at low concentrations, they can cause great harm to human health and ecological environment [6,7]. Therefore, strict control of VOCs emissions is necessary. Generally speaking, VOCs emissions have the following characteristics, such as large air volume, low VOCs concentrations and water containing [8-10]. Adsorption has been considered as an effective method to remove VOCs because of its high removal efficiency, low energy and low operation cost [11-13]. The core of the adsorption technology is the adsorbent. Activated carbons and molecular sieve are the most widely used adsorbent for VOCs [14]. Activated carbons have excellent performance in VOCs adsorption because of its multistage pore structure and large specific surface area. However, its irregular pore structure and poor thermal stability make its regeneration process complicated, difficult and dangerous [15,16]. Compared with the activated carbon, the molecular sieves are the commonly used adsorbents in the process of removing VOCs due to their high adsorption capacity, high thermal stability, low cost and easy recycling.

ZSM-5 is a promising option for VOCs adsorption. However, the presence of moisture in the VOCs gas can greatly decrease the adsorption capacity of the adsorbent because a part of the adsorbed VOCs will be replaced by water molecules [17-19]. Actually, the ZSM-5 molecular sieve with high Si/Al ratio and even pure silicate does have a high hydrophobicity [20]. However, its high price limits its use because existing synthetic method often required adding crystals, surfactants and expensive organic templates [21,22]. The ZSM-5 molecular sieve with low Si/Al ratio is highly hydrophilic, which is NOT an ideal adsorbent for VOCs control and needs to be modified. Generally, there were several modification methods to improve the water resistance of molecular sieve, which were acid de-alumination, silanization, impregnation and cation modification [23-26]. Traditional researches had always focused on separate modification methods, and its adsorption capacity increase is very limited. With an aim to improve the adsorption capacity of VOCs and reduce the adsorption capacity of water, ZSM-5 molecular sieve could be tailored by combination modification methods. In this paper, toluene was used as a model of VOCs, and the ZSM-5 molecular sieve (Si/Al = 36) was selected as the raw material. The ZSM-5 molecular sieve was modified by combination modification methods, and its adsorption properties and mechanism were studied.

Experimental Section

Preparation of Modified ZSM-5

Modification of ZSM-5 molecular sieve was conducted by acid de-alumination followed by silanization. Firstly, 3 g ZSM-5 molecular sieve was mixed with HCl (different concentration) at some ratio [27,28]. The reaction was conducted at 373 K and stirred under reflux for several hours. After the reaction, the product was aspirated, washed with deionized water, and centrifuged several times until the solution pH was 7. The resulting ZSM-5 molecular sieve was dried at 393 K for 12 h. Secondly, acid treated ZSM-5 molecular sieve 1.5 g was used for the silanization modification [29-31]. Silanization was conducted with different amounts of TMCS using toluene as a dispersant. The experiment was conducted at different temperatures with reflux for 5 h. After the reaction, the experiment was extracted and filtered with C2H5OH, and then filtered and dried in a 373 K vacuum drying chamber for 1h. Thirdly, the modified ZSM-5 molecular sieves were calcined at 823 K for 4 h in a tubular furnace. All adsorbent materials were tableted and kept isolated in a desiccator.

Competitive Adsorption Breakthrough Experiments

The competitive adsorption breakthrough experiments were carried out with a fixed bed, as listed in Figure 1. Gaseous toluene and water vapor were generated by two micro-injection pumps, and N2 was used as the carrier gas controlled by a mass flow controller (S48-32, HORIBA Precision Instruments). The concentrations of water vapor and toluene were quantified using the dew point meter (HQ-FTD-2DAC, Beijing Qinghong Co. Ltd) and the fixed gas PID detector (APEG-TH2S-G-2N, Shenzhen Anpaer Co. Ltd.). Approximately 1 g tablet adsorbent was put into a quartz tube with an inner diameter of 8 mm and a length of 25 mm. Adsorption was conducted at ambient pressure and 308 K, which was controlled by an electric furnace temperature controller. In the competitive adsorption breakthrough experiment, the zero-time was determined by the blank test. The breakthrough point was respectively determined at the concentration of adsorbent in outlet gas reached 5 % of the each component in the feed. The tail gas was discharged outside after treatment. Regeneration was carried out with N2 as the regeneration gas. The relative error of the competitive adsorption experiment was lower than ± 5 %.

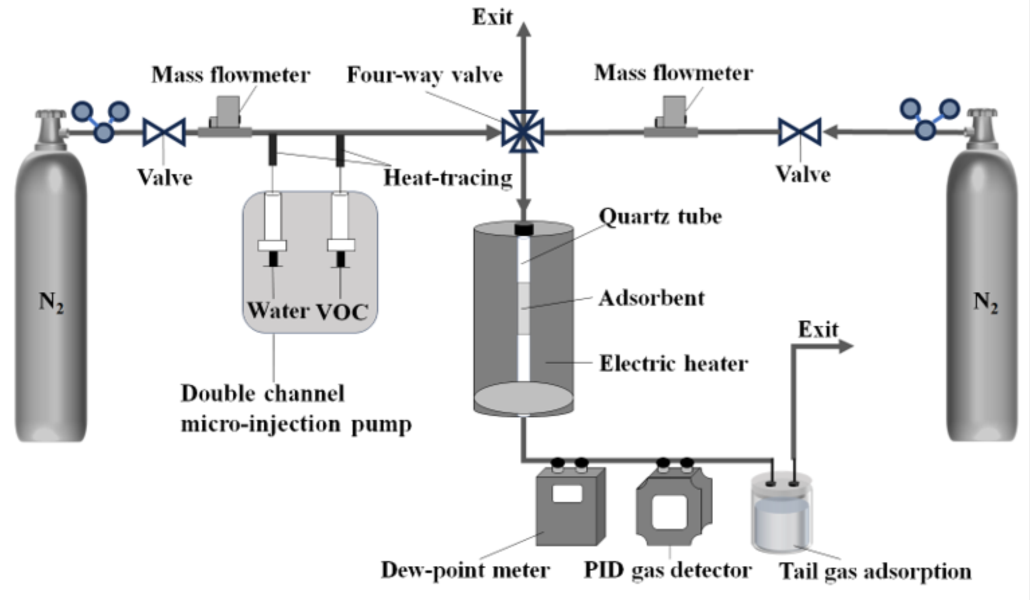

Figure 1: Schematic diagram of toluene/moisture competitive adsorption/desorption.

Results and Discussions

XRD Results

The XRD patterns showed the structures of the ZSM-5 molecular sieve before and after modification, as listed in Figure 2. For either the raw ZSM-5 molecular sieve or the modified ZSM-5 molecular sieve, all samples had characteristic peaks at 7.9°, 8.8°, 23.1° and 23.9°, corresponding to (101), (200), (501), (151) and (303), indicating that all samples presented a typical MFI structure and good crystallinity, even after HCl dealumination and silanization [32,33]. Figure 2a illustrated the effect of HCl concentration on structures of the ZSM-5 molecular sieve. In contrast to the raw ZSM-5 molecular sieve, the peak strength increased after HCl de-alumination. In this modification, part of Al was successfully removed from the ZSM-5 molecular sieve, and Si/Al ratio increased accordingly. Different HCl concentration had different effect on ZSM-5 structures. When HCl concentration was 2.0 mol/L, some Al on non-skeleton of ZSM-5 molecular sieve was gently removed, and the modified skeleton structure was preserved well. As listed in Figure 2a, the characteristic peak intensity of the modified ZSM-5 molecular sieve increased obviously, and the modified ZSM-5 molecular sieve had better relative crystallinity. When HCl concentration increased to 4.0 mol/L and 6.0 mol/L, the remove of Al from ZSM-5 molecular sieve became violently. Not only Al on non-skeleton was removed from ZSM-5 molecular sieve, but also Al on skeleton was removed too.

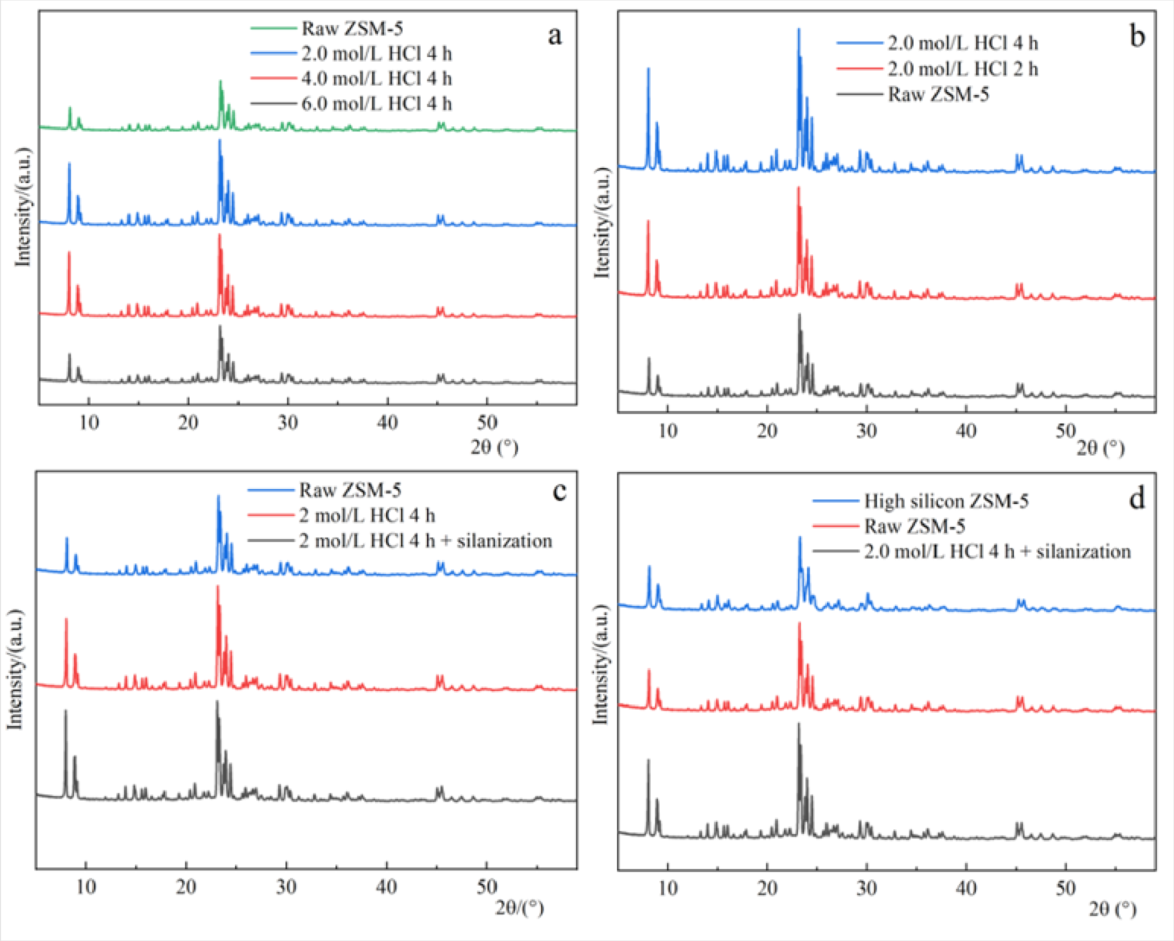

Figure 2: XRD results of ZSM-5 with and without modification.

a. Effect of HCl concentration on ZSM-5 structure
b. Effect of HCl de-alumination time on ZSM-5 structure
c. Effect of modification on ZSM-5 structure
d. Effect of combined modification on ZSM-5 structure.

Compared with the ZSM-5 molecular sieve modified by 2.0 mol/L HCl, the crystal structure of the ZSM-5 molecular sieve modified by 4.0 mol/L or 6.0 mol/L HCl became a little worse. Compared with the raw ZSM-5 molecular sieve, there was no obvious amorphous peaks found in XRD patterns of the modified the ZSM-5 molecular sieve samples even after 6 mol/L HCl de-alumination, indicating that the ZSM-5 molecular sieve structure was stable. Figure 2b showed the effect of HCl de-alumination time on the structure of the ZSM-5 molecular sieve. With the longer de-alumination time, 2 mol/L HCl removed Al on non-skeleton gently and continuously from the surface to the inner part of ZSM-5 molecular sieve, leading to the modified ZSM-5 molecular sieve showed a better crystal form, and the characteristic peaks intensity at 7.9°, 8.8°, 23.1° and 23.9° gradually increased. Figure 2b showed the framework structure was orderly and the topology was continuous. Moreover, with the extension of de-aluminization time, self-adjustment maybe occurred inside the ZSM-5 molecular sieve, which made the crystal more regular. Figure 2c listed the effect of modification on ZSM-5 structure. Compared with ZSM-5 de-aluminated by 2.0 mol/L HCl for 4 h separately, ZSM-5 modified by combination methods showed good crystallinity too. Furthermore, with the increase of Si/Al ratio, the characteristic peak intensity at 7.93° (101) and 8.79° (020) increased obviously, while the other characteristic peak intensity was unchanged. The result was in good agreement with Zhang, et al. [34], they ascribed the strong peak at 7.93° to that the ZSM-5 particles have more morphology, and ascribed the strong diffraction peak at 8.79° to the presence of (020) crystal surface. Figure 2d recorded the effect of combined modification on ZSM-5 structure. Compared with raw ZSM-5 and high silicon ZSM-5, the ZSM-5 modified by combined methods showed relative better crystallinity.

FTIR Results

The FTIR spectra of the ZSM-5 molecular sieves before and after modification were shown in Figure 3. The absorption peak at 3429-3450 cm-1 is the stretching vibration of O-H, and the absorption peak at 1640 cm-1 is the bending vibration of O-H. The absorption peak at 1090 cm-1 belongs to the asymmetric stretching vibration of T-O-T (T refers to Si or Al), the absorption peak at 801 cm-1 is the symmetric stretching vibration of T-O bond, and the absorption peak at 459 cm-1 refers to the bending vibration of T-O bond. These three absorption peaks belong to the vibration band of inner tetrahedron [35,36]. It is generally believed that the absorption fingerprint peak at 556 cm-1 is closely related to the structural unit characterized in the molecular sieve skeleton, and can be attributed to the chain structures caused by SiO4 and AlO4 [37]. The absorption peak near 1229 cm-1 is slightly increased with the increasing wave of the Si/Al ratio and the peak becomes weaker. This is due to the fact that the Al-O bond (0.175 nm) is longer than the Si-O bond (0.161 nm), leading to a smaller chemical bond force constant than the Si-O bond. As the Si/Al ratio increased, the stretching vibration absorption peak of the T-O-T structure decreased. For either the raw ZSM-5 molecular sieve or the modified ZSM-5 molecular sieve, the absorption peak at 556 cm-1 is attributed to the chain structures caused by SiO4 and AlO4, and the results were in good agreement with the XRD results.

Figures 3a & 3b illustrated the effect of HCl concentration on structures of the modified ZSM-5 molecular sieves. For the raw ZSM-5 molecular sieve, the stretching vibration of O-H at 3429-3450 cm-1 showed an intense band, indicating there were many O-H in raw ZSM-5 molecular sieve, which was in good agreement with its hydrophilicity. After HCl de-alumination, the stretching vibration peak of O-H at 3429-3450 cm-1 and bending vibration peak of O-H at 1640cm-1 showed a lower intense band, indicating there were few O-H in modified ZSM-5 molecular sieve. The decrease of O-H led to its hydrophobic. After HCl de-alumination, as expected, Al on ZSM-5 molecular sieve decreased. As the Si/Al ratio increased, the modified ZSM-5 molecular sieve showed hydrophobic, which in good agreement with the previous report [38]. Figure 3c illustrated the effect of de-aluminated time on FTIR spectra of ZSM-5 molecular sieve. For 2 mol/L HCl, as the de-aluminated time increased, Al on non-skeleton decreased gently and continuously, leading to Si/Al ratio increased continuously, and the O-H decreased continuously. The result matched well with the XRD results. While for 4 mol/L HCl and 6 mol/L HCl, as the de-aluminated time increased, Al on non-skeleton and Al on skeleton decreased, but the O-H sometimes decreased relatively smaller.

Figure 3d listed the effect of different modified methods on structures of ZSM-5 molecular sieves. It was clear that the stretching vibration peak of O-H changed dramatically. Compared with the raw ZSM-5 molecular sieve, the stretching vibration peak of O-H at 3429-3450 cm-1 and the bending vibration peak of O-H at 1640 cm-1 decreased obviously after HCl de-alumination. After HCl de-alumination followed by silanization, the stretching vibration peak of O-H decreased further. From Figure 4d, as the Si/Al ratio increased, the stretching vibration peak at near 1229 cm-1 became weaker, which belonged to T-O-T structure and had relationship with Si/Al ratio.

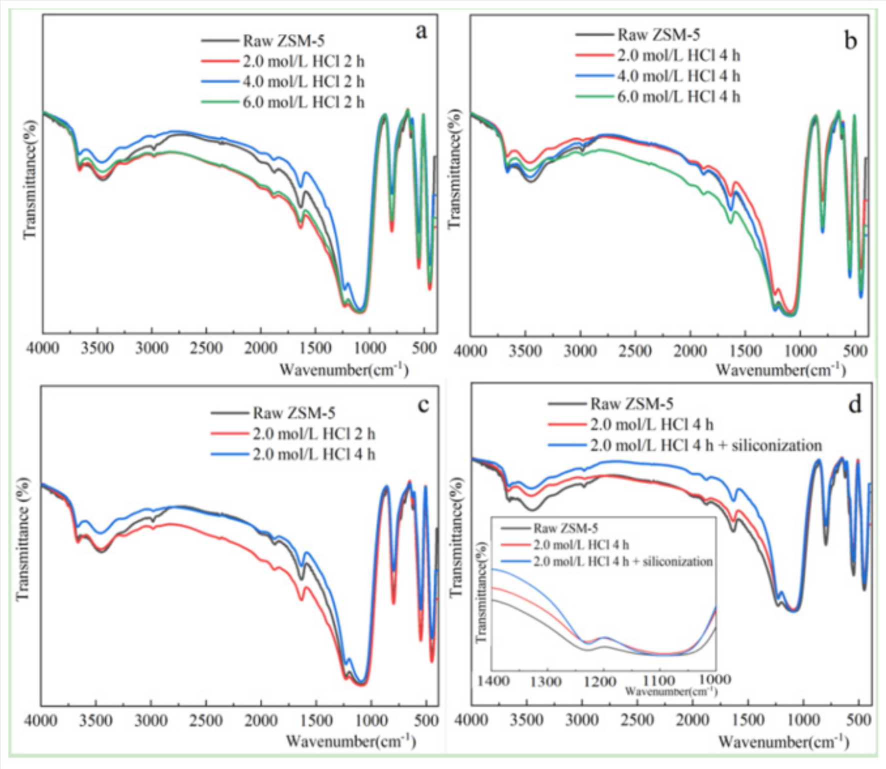

Figure 3: FTIR spectra of modified ZSM-5 molecular sieve.

a. de-aluminated with different concentration of HCl for 2 h
b. de-aluminated with different concentration of HCl for 4 h
c. ZSM-5 molecular sieve de-aluminated for different time
d. ZSM-5 molecular sieve modified by different methods.

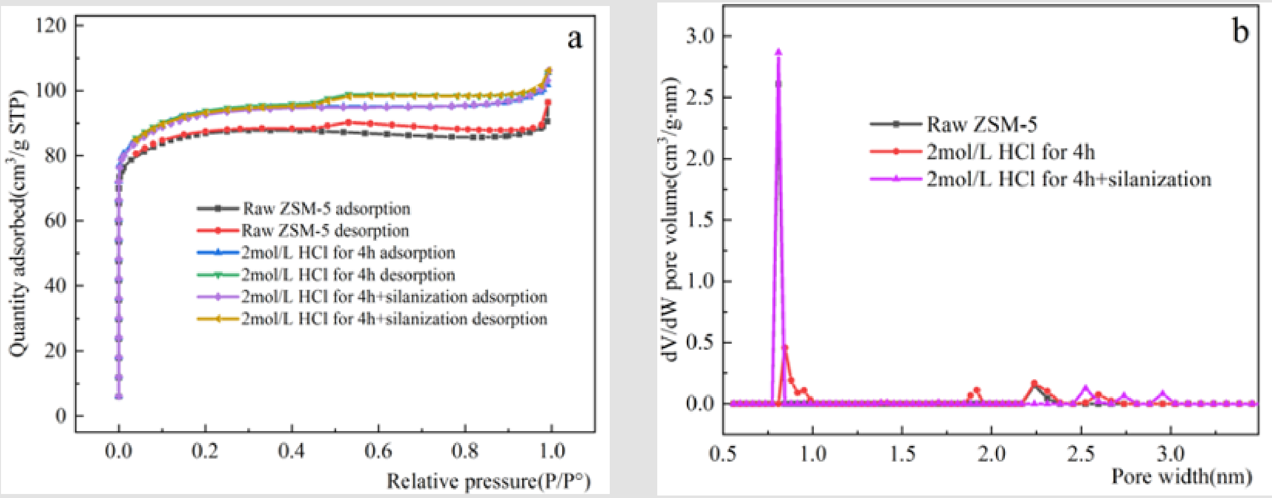

Figure 4:

a. N_2 adsorption-desorption equilibrium isotherms of ZSM-5 before and after modification
b. Pore size distribution of ZSM-5 before and after modification.

SEM Results

Figure 5 showed the SEM images of ZSM-5 before and after modification. As illustrated in Figure 5a, the raw ZSM-5 molecular sieve had a prismatic structure and a smooth surface, indicating that raw ZSM-5 molecular sieve had a good crystallinity. Figures 5b-5e showed the SEM images of ZSM-5 modified by HCl. When HCl concentration was relatively low, the structure of the modified ZSM-5 still maintained the prismatic and smooth surface, either for 2 h or for 4 h modification. As HCl concentration increased, the surface of the modified ZSM-5 became rough, and even there were some cracks appeared on the surface. The modification by different HCl concentration could affect the pore size and specific surface area of the modified ZSM-5 molecular sieve, which was in good agreement with the BET results. Figure 5f showed the SEM image of ZSM-5 after 2 mol/L HCl de-alumination for 4 h followed by silanization. It was clear that the surface was still smooth and crystallinity maintained well. From Figure 5f, it was also found that the ZSM-5 molecular sieve particles had more morphology, which made the XRD diffraction peak increased at 8.79°.

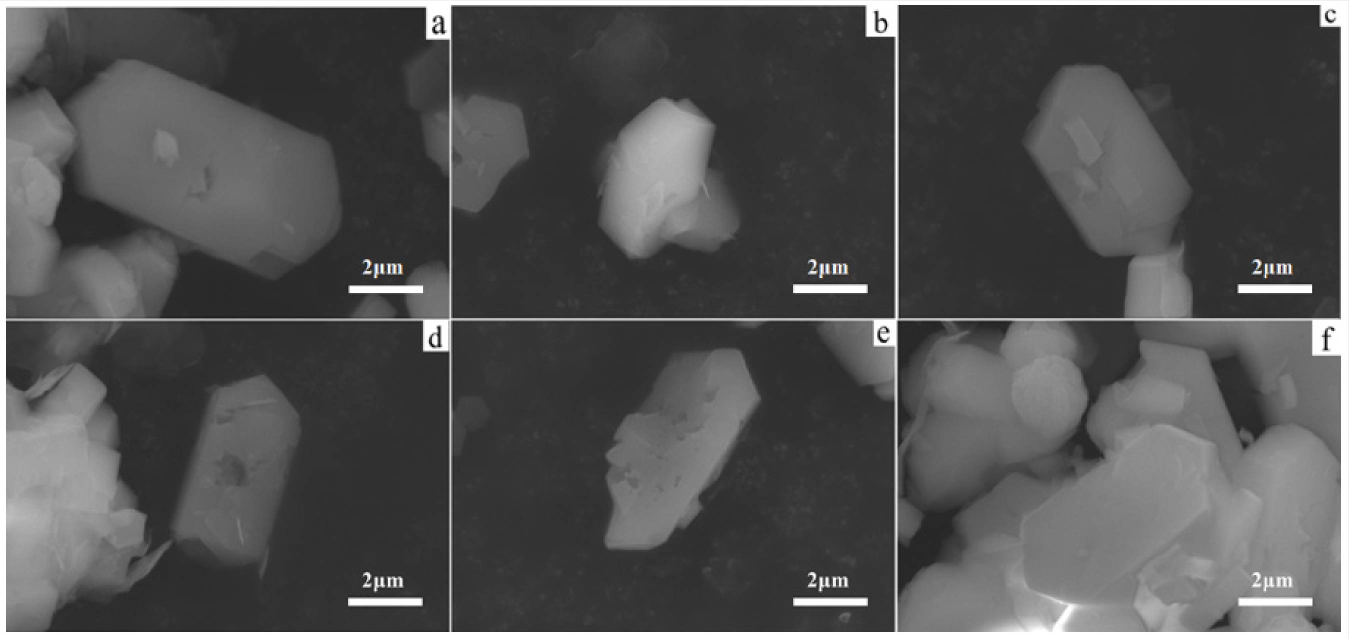

Figure 5: SEM images of ZSM-5 before and after modification.

a. Fresh ZSM-5
b. ZSM-5 2 mol/L HCl de-alumination for 2 h
c. ZSM-5 treated in 2 mol/L HCl de-alumination for 4 h
d. ZSM-5 treated in 4 mol/L HCl de-alumination for 4 h
e. ZSM-5 treated in 6 mol/L HCl de-alumination for 4 h
f. ZSM-5 treated in 2 mol/L HCl de-alumination for 4 h followed by silanization.

BET Results

To further understand the effect of combined modification on structures of ZSM-5 molecular sieve, BET analysis was performed and the results were illustrated in Figure 4. Figures 4a & 4b demonstrated the N2 adsorption/desorption equilibrium isotherms (BET) and pore size distribution of ZSM-5 molecular sieves before and after modification. According to IUPAC, all the adsorption/desorption isotherms of N2 on the adsorbents were of type I, indicating that the adsorbents were rich in micro-pores, and mono-layers adsorption were formed on the surface of the adsorbents [39,40]. For the raw ZSM-5 molecular sieve, the surface area was as high as 96 m3/g and the micropore diameter was about 0.6 nm. Compared with the raw ZSM-5 molecular sieve, after HCl de-alumination, the surface area increased to 108 m3/g, the micropore decreased dramatically, while the mesopores with different pore size increased obviously. This result was due to the effect of HCl on the pore expanding. As for combined modified ZSM-5 molecular sieve, after HCl de-alumination followed by silanization, the surface area maintained at about 108 m3/g. As for the pores of the ZSM-5 modified by the combined methods, in addition to maintaining the small amount of mesopores with different pore sizes, a lot of micropores reappeared due to the silanization of ZSM-5, and the pore size decreased to the size of the original molecular sieve.

The traditional molecular sieve only had microporous channels, which led to the long path for toluene diffusion in the molecular sieve and low adsorption rate. The realization of pore multistage could shorten the mass transfer path through the introduction of medium/micro pore, increased the specific surface area and pore capacity, improved the VOC adsorption rate and increased the adsorption capacity. In summary, the introduction of multistage pores not only reduced diffusional resistances, resulting in rapid adsorption, but also increased the surface area, resulting in the high adsorption capacity. The BET surface area, the pore volume and the average pore size of the ZSM-5 molecular sieve before and after modification were summarized in Table 1. Compared with the raw ZSM-5 molecular sieve, after HCl de-alumination, the surface area increased apparently from 333.7 m2/g to 355.3 m2/g, and the average pore diameter increased from 3.34 nm to 3.75 nm. HCl de-alumination not only improved the Si/Al ratio of ZSM-5 molecular sieve, but also changed the pore size and pore distribution. The increase of Si/Al ratio improved the hydrophobicity. The optimal pore distribution could enhance the mass transfer in the adsorbent and improve the adsorption amount. After HCl de-alumination followed by silanization, the average surface area showed no remarkable loss.

Table 1: Physical adsorption parameters of ZSM-5 molecular sieve before and after modifications.

Adsorbents	Surface area (m^2/g)	Pore volume (cm^3/g)	Pore size (nm)
Raw ZSM-5	333.7	0.1065	3.34
ZSM-5 after HCl dealumination	355.3	0.1100	3.76
ZSM-5 after HCl dealumination followed by silanization	352.6	0.1085	3.40

However, the pore diameter decreased down to the size of the raw ZSM-5 molecular sieve, the optimal pore distribution could still enhance mass transfer in the adsorbents for toluene, which was favour to toluene adsorption. In addition, HCl de-alumination was important to the following silanization because it enlarged the pore size and provided much more space for subsequent silanization. As we all known, when TMCS was grafting to ZSM-5 molecular sieve, silanization modification could cause a decrease in pore size and specific surface area, and damage part of its pore structure. Thus, the prior HCl de-alumination before silanization was critical in ZSM-5 modification. Similar to the traditional modification, the silanization could act with -OH in ZSM-5 molecular sieve to improve the hydrophobicity. As for the silanization of the raw ZSM-5 molecular sieve, the silanization group maybe only grafted to the outer surface of the raw ZSM-5 molecular sieve, resulting in a limited improvement of hydrophobicity. Alternatively, it was possible that the silanization groups not only grafted to the outer surface of the molecular sieve, but also to the inner pores of ZSM-5. Unfortunately, the silanization group may block the micropores of the raw ZSM-5, which reduced the adsorption amount of water and toluene simultaneously. The solution to the above trouble can be the combined methods. The previous HCl de-alumination not only increased the specific surface area, but also expanded the pore size. Wider pores could reduce diffusional resistances, resulting in rapid adsorption.

The latter silanization occured not only on the outer surface, but also in the inner hole, and the silanization inside the hole did not block the hole. The result was that not only the hydrophobicity was improved, but also the adsorption amount of toluene was greatly increased. In addition, HCl de-alumination introduced multistage pores to ZSM-5, and the introduction of multistage pores not only greatly improved the rate of toluene, but also increased the adsorption capacity of toluene [41-43]. In summary, the increasing toluene adsorption amount was explained by increased specific surface area, appearce of multistage pores and the higher hydrophobicity, and the higher hydrophobicity came from both HCl de-alumination and silanization of ZSM-5 molecular sieve [44,45].

ICP Results

The concentration of Si, Al element in ZSM-5 molecular sieve before and after modification was listed in Table 2. Compared with the raw ZSM-5 molecular sieve, Si/Al ratio increased from 36.7 to 51.04 after modification. It is reasonable that the higher Si/Al ratio has higher hydrophobiciy. The competitive adsorption experiment showed that, the modified ZSM-5 molecular sieve with high Si/Al ratio had unique toluene selective adsorption ability because of its excellent hydrophobicity. This result is in accordance with the previous work [46].

Table 2: ICP of ZSM-5 before and after modification.

Sample	Si (mg/kg)	Al (mg/kg)	Si/Al
Raw ZSM-5	50669.82	1379.04	36.7
Modified ZSM-5	91948.53	1801.47	51.04

Competitive Breakthrough Adsorption

Water vapour is omnipresent in VOCs and humidity has obvious impact on the adsorption, so the competitive breakthrough adsorption is carried out to investigate the property of ZSM-5 molecular sieve before and after modification. Figure 6 showed the effect of modification on the adsorption performance of ZSM-5 molecular sieve. First of all, the raw ZSM-5 molecular sieve showed a high hydrophily and a low toluene adsorption capacity. In humid toluene stream, the water vapor breakthrough capacity of the raw ZSM-5 molecular sieve was 7.87 %, while the toluene breakthrough capacity was only 1.87 %. High hydrophily always has a negative impact on the toluene adsorption capacity of the ZSM-5 molecular sieve, because the adsorbed water vapor can occupy the active sites of the molecular sieve, reducing the adsorption capacity of the adsorbent for toluene [47,48]. Some researchers even found that the “roll over” phenomenon occurred in the adsorption process, and moisture could replace the adsorbed toluene, which also reduced the adsorption capacity of toluene [49,50]. Silylation reactions have been widely used to modify the property of molecular sieves. In this paper, trimethyl chlorosilane (TMCS) was selected as the silanization reagent and grafted onto the ZSM-5 molecular sieve. Unfortunately, only grafting TMCS to ZSM-5 molecular sieve did not achieve the desired effect.

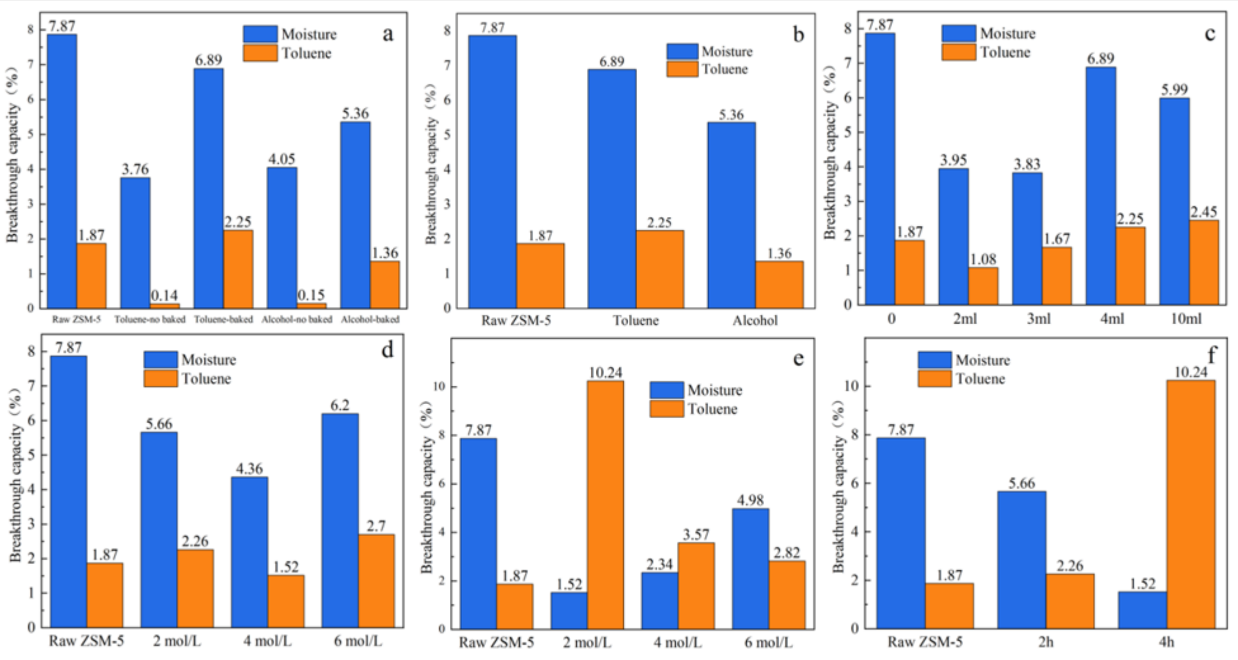

Figure 6: Effect of modification on adsorption performance of ZSM-5.

a. Effect of bake on performance of ZSM-5 (silanization)
b. Effect of solvent on performance of ZSM-5 (silanization)
c. Effect of silylation amount on performance of ZSM-5 (silanization)
d. Effect of HCl concentration on performance of ZSM-5 (2 h HCl + silanization)
e. Effect of HCl concentration on performance of ZSM-5 (4 h HCl + silanization)
f. Effect of HCl dealumination time on performance of ZSM-5 (2 mol/L HCl + silanization).

As listed in Figure 6a, the water absorption and toluene adsorption of the modified ZSM-5 molecular sieve were significantly reduced simultaneously. Therefore, the bake experiment was attempted after the silaniazation reaction. Figure 6a showed the effect of bake on adsorption performance of ZSM-5 molecular sieve. After silylation reaction, the adsorption capacity of unbaked ZSM-5 molecular sieve was small, while the adsorption capacity of baked ZSM-5 molecular sieve was improved. The reason would be that the silanization group grafting to ZSM-5 molecular sieve blocked some pores of the molecular sieve, so either toluene or moisture could NOT penetrate into the internal pores of the molecular sieve. After baking, some -CH3 of TMCS volatiled from ZSM-5, leading to a little adsorption rebound of the moisture and toluene. Figure 6b showed the effect of solvent on performance of ZSM-5. In silanizing reaction, when benzene was used as the solvent, the performance of ZSM-5 was better than alcohol as the solvent. Benzene was preferred as the solvent because benzene was a nonpolar solvent. Figure 6c showed the effect of TMCS amount on performance of ZSM-5. As TMCS amount increased, the moisture adsorption capacity of the modified ZSM-5 decreased while the toluene adsorption capacity increased. Comparing the toluene adsorption capacity of raw ZSM-5 and modified ZSM-5, it is clear that the hydrophobic character play an important role.

At the same time, the above results indicated that the separate modification had a very limited effect, and it was necessary to attempt the combination modification methods. Due to size exclusion effects and diffusion constraints, grafting of TMCS to ZSM-5 molecular sieve is confined to the outer surface and pore mouths, and internal functionalization of molecular sieve is limited [51,52]. Before silanization modification, HCl de-alumination was carried out to remove Al on non-skeleton of ZSM-5 molecular sieve. HCl de-alumination not only improved Si/Al ratio, but also broadened the pore size, which made it an attractive option for ZSM-5 modification. Figure 6d listed the effect of HCl concentration on performance of ZSM-5 in combination modification. The results showed that high concentration of HCl modified ZSM-5 molecular sieve violently. It could not only remove Al on the non-skeleton of ZSM-5 molecular sieve, but also remove Al on the skeleton. The result caused a reduced crystallinity of the ZSM-5 molecular sieve, and even reduced the specific surface area of the ZSM-5 molecular sieve. With HCl de-alumination time increase, this effect became obvious. On the contrary, the low concentration of HCl de-alumination showed a very good modification effect. From the surface to the center of the ZSM-5 molecular sieve, the low concentration HCl removed Al on the non-skeleton gently and continuously, which not only improved the crystallinity of ZSM-5 molecular sieve, but also broadened the pore size of ZSM-5 molecular sieve.

After combined modification, the competitive breakthrough adsorption of toluene and water vapor showed that there was a dramatic shift from hydrophilic to hydrophobic properties. As listed in Figure 6e, the water vapour adsorption capacity dropped to only 1.52 %, while toluene breakthrough capacity achieved at 10.24 %. Hence, the moisture adsorption capacity decreased by 80.7 % while the toluene capacity increased by 547.6 %, compared with the raw ZSM-5 molecular sieve. In summary, in ZSM-5 modification, various parameters were significant, such as hydrophobic properties, Si/Al ratio, pore size and specific surface area, which affected the adsorption performance of ZSM-5 molecular sieve comprehensively [53]. Figure 6f summarized the effect of 2 mol/L HCl de-alumination time on adsorption performance of ZSM-5 molecular sieve. As de-alumination time increased, the moisture adsorption capacity decreased continuously, while the toluene adsorption capacity increased continuously. Comparing the toluene adsorption capacity of raw ZSM-5 molecular sieve and modified ZSM-5 molecular sieve, it was concluded that the hydrophobic character, the high Si/Al ratio, the specific surface area and even the pore size played an important role, and further investigation was needed.

DFT Calculations for Adsorption Mechanism

To investigate the adsorption mechanism at an atomic level, the ZSM-5(1 0 0) crystal plane and its corresponding adsorption configuration were constructed (Figures 7a & 7b), followed by structural optimization using the CP2K computational package. The calculations were performed at the Perdew–Burke–Ernzerhof (PBE) level of theory with the DZVP-MOLOPT-SR-GTH basis set. Frontier molecular orbital analysis revealed that the lowest unoccupied molecular orbital (LUMO) of the ZSM-5(1 0 0) surface was predominantly localized on the upper region (Figure 7c), whereas the highest occupied molecular orbital (HOMO) was distributed across the lower region (Figure 7e). This observation suggests that the vacant orbitals on the ZSM-5 surface exhibit electron-accepting capability, facilitating interactions with toluene molecules. For the adsorption system, the unoccupied orbitals were concentrated on the adsorbed toluene molecule (Figure 7d), while the occupied orbitals were primarily associated with oxygen and silicon atoms in the zeolite framework (Figure 7f). These findings corroborate the electron transfer mechanism from the toluene molecule to the ZSM-5(1 0 0) surface upon coordination, highlighting the role of orbital hybridization in stabilizing the adsorption complex.

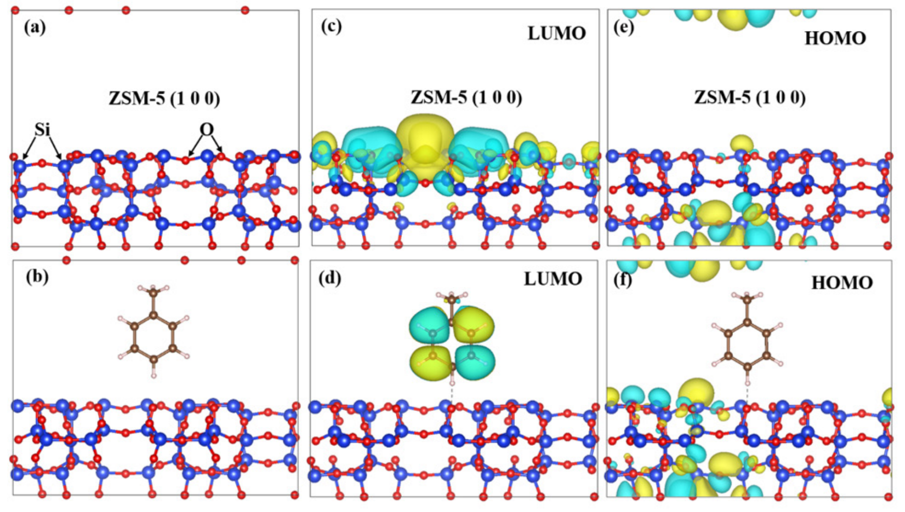

Figure 7: Crystal structure of

a. ZSM-5 (1 0 0) crystal plane and
b. toluene adsorbed by ZSM-5 (1 0 0) crystal plane
c. LUMO and
d. LUMO of ZSM-5 (1 0 0) crystal plane
e. LUMO and
f. LUMO of toluene adsorbed by ZSM-5 (1 0 0) crystal plane. CP2K, PBE // DZVP-MOLOPT-SR-GTH.

Conclusions

Adsorption is an efficiency method to remove VOCs. The hydrophilicity of the ZSM-5 molecular sieve limits its application in VOCs adsorption. In this paper, ZSM-5 molecular sieve was successfully modified by combination modification methods, and the modified ZSM-5 exhibited both high toluene adsorption capacity and good hydrophobicity. Single desalinization and silanization modification had limited effect on ZSM-5, while the combination modification was conducted successfully. The combination modification was conducted by acid de-alumination followed by silanization. The competitive adsorption breakthrough experiment found that, compared with the raw ZSM-5 molecular sieve, the water adsorption capacity of the modified ZSM-5 molecular sieve decreased from 7.87 % to 1.52 %, and toluene adsorption capacity improved from 1.87 % to 10.24 %. Combination modifications were monitored by XRD, FTIR, BET et al., the hydrophobicity, specific surface area, pore size and pore distribution were the critical factors affecting the VOCs adsorption of the ZSM-5 molecular sieve. The modification of ZSM-5 was inexpensive, which make it attractive for commercial application.

Funding

This work is performed by School of Chemistry and Chemical Engineering, Henan Key Laboratory of Green Coal Conversion, Distinguished Foreign Scientist Workshop on Coal Green Conversion (GZS20200012), Henan Polytechnic University for AramcoTech, under the framework of a contract of AramcoTech 2019-017/3.

Notes

The authors declare no competing financial interest.

References

1. Wu P, Jin X, Qiu Y, Ye D (2021) Recent Progress of Thermocatalytic and Photo/Thermocatalytic Oxidation for VOCs Purification over Manganese-based Oxide Catalysts. Environ Sci Technol 55(8): 4268-4286.
2. Wang Y, He J, Li X, Wang M, Zhou Y, et al. (2021) Low Temperature Combustion of VOCs with Enhanced Catalytic Activity over MnO_2 Nanotubes Loaded with Pt and Ni-Fe Spinel. ACS Appl Mater Interfaces 13(39): 46830-46839.
3. Xu W, Song L, Jin H, Jin D, Wei X, et al. (2024) A luminescent binuclear Cu(I) complex constructed by bipyridine, TD-DFT calculation, and its fluorescent sensing properties for VOCs. J Molecular Structure 1318(Part 1): 139283.
4. Jung S, Fang J, Chadha T S, Biswas P (2018) Atmospheric Pressure Plasma Corona Enhanced by Photoionizer for Degradation of VOCs. J Phys D: Appl Phys 51(44): 445206.
5. Chen Y, Liu H (2002) Absorption of VOCs in a Rotating Packed Bed. Ind Eng Chem Res 41(6): 1583-1588.
6. Kamal M S, Razzak S A, Hossain M M (2016) Catalytic Oxidation of Volatile Organic Compounds (VOCs)–A Review. Atmospheric Environment 140: 117-134.
7. Meininghaus CKW, Prins R (2000) Sorption of Volatile Organic Compounds on Hydrophobic Zeolites. Microporous Mesoporous Mater 35(6): 349-365.
8. Kim Y, Harrad S, Harrison R (2001) Concentrations and Sources of VOCs in Urban Domestic and Public Microenvironments. Environ Sci Technol 35(6): 997-1004.
9. Li J, Ma X, Wu H, Yang L (2021) Adsorption of Low-Concentration VOCs on Modified Activated Carbons in a Humid Atmosphere. Energy Fuels 35(6) 5090-5100.
10. Yu F, Luo L, Grevillot G (2002) Adsorption Isotherms of VOCs onto an Activated Carbon Monolith: Experimental Measurement and Correlation with Different Models. J Chem Eng Data 47(3): 467-473.
11. Villora-Picó JJ, Coloma-Pascual F, Sepúlveda-Escribano A, Pastor-Blas MM (2024) N-doped Activated Carbons Obtained from Polyaniline for Toluene and Water Adsorption. Inorganic Chemistry Communications 167: 112684
12. Dobre T, Parvulescu OC, Iavorschi G, Stroescu M, Stoica A, et al. (2014) Volatile Organic Compounds Removal from Gas Streams by Adsorption onto Activated Carbon. Ind Eng Chem Res 53: 3622-3628.
13. Kraus M, Trommler U, Holzer F, Kopinke F, Roland U, et al. (2018) Competing Adsorption of Toluene and Water on Various Zeolites. Chem Eng J 351: 356-363.
14. Drobek M, Figoli A, Santoro S, Navascues N, Motuzas J, et al. (2015) PVDF-MFI Mixed Matrix Membranes as VOCs Adsorbers. Microporous Mesoporous Mater 207: 126-133.
15. Cardoso B, Mestre A, Carvalho A, Pires J (2008) Activated Carbon Derived from Cork Powder Waste by KOH Activation: Preparation, Characterization, and VOCs Adorption. Ind Eng Chem Res 47(16): 5841-5846.
16. Zhang X, Gao B, Creamer AE, Cao C, Li Y, et al. (2017) Adsorption of VOCs onto Engineered Carbon Materials: A review. J Hazard Material 338: 102-123.
17. Xu WQ, He S, Lin CC, Qiu YX, Liu XJ, et al. (2018) A Copper Based Metal-organic Framework: Synthesis, Modification and VOCs Adsorption. Inorganic Chemistry Communications 92: 1-4.
18. Karimah N, Mahardika A, Utomo W, Rozafia A, Afifah P, et al. (2025) Preparation of Titanium Dioxide/Graphitic Carbon Nitride Heterostructure Anchored on Hierarchical ZSM-5 for Synergistic Adsorptive and Photocatalytic Dye Degradation. J Molecular Structure 1335: 141968.
19. Bauville G, Heninger M, Lemaire J, Jeanney P, Santos Sousa J, et al. (2025) VOCs conversion in He/H_2O plasma produced in a micro-capillary tube at atmospheric pressure. J Phys D: Appl. Phys 58: 015207.
20. Ji X, Zhou Q, Zhang X (2025) Effect of the Synthesis and Post-Treatment of Twin-Crystal ZSM-5 Zeolites on Their VOCs Adsorption Performance. Ind Eng Chem Res 64: 61-70.
21. Yue X, Wang S, Li D, Zhao Y, Wang S, et al. (2023) Experimental and Numerical Investigations on the Adsorption/Desorption Performance of Low-Concentration VOCs over H-ZSM-5 with Different SiO_2/$Al2O_3$ Ratios. Ind Eng Chem Res 62: 5408-5419.
22. Yue Y, Kan Y, Bai Y, Gu L, Liu H, et al. (2018) Seed-assisted, Template-free Synthesis of ZSM-5 Zeolite from Natural Aluminosilicate Minerals. Applied Clay Science 158: 177-185.
23. Pasti L, Rodeghero E, Sarti E (2016) Competitive Adsorption of VOCs from Binary Aqueous Mixtures on Zeolite ZSM-5. RSC Advances 6: 54544-54552.

24. Li X, Zhang L, Yang Z (2020) Hydrophobic Modified Activated Carbon Using PDMS for the Adsorption of VOCs in Humid Condition. Separation and Purification Technology 239: 116517-116517.

25. Zhao Y W, Shen B X, Sun H (2016) Chemical Liquid Deposition Modified ZSM 5 Zeolite for Adsorption Removal of Dimethyl Disulfide. Ind Eng Chem Res 55: 6475-6480.

26. Qian XC, Bai GZ, He P P, Fei Z Y, Liu Q, et al. (2018) Rapid CO_2 Adsorption over Hierarchical ZSM-5 with Controlled Mesoporosity. Ind Eng Chem Res 57(49): 16875-16883.

27. López-Fonseca R, Rivas B D, Gutiérrez-Ortiz JI, Aranzabal A, González-Velasco JR, et al. (2003) Enhanced Activity of Zeolites by Chemical Dealumination for Chlorinated VOC Abatement. Applied Catalysis 41(1–2): 31-42.

28. Shen X Q, Du XS, Yang DF, Ran JY, Yang ZQ, et al. (2021) Influence of Physical Structures and Chemical Modification on VOCs Adsorption Characteristics of Molecular Sieves. Journal of Environmental Chemical Engineering 9: 1-7.

29. Han X, Wang L, Li J (2011) Tuning the Hydrophobicity of ZSM-5 Zeolites by Surface Silanization Using Alkyltrichlorosilane. Applied Surface Science 257(22): 9525-9531.

30. Alonso-Doncel M, Peral A, Shamzhy M, Čejka J, Sanz R, et al. (2020) Untangling the Role of the Organosilane Functional Groups in the Synthesis of Hierarchical ZSM-5 Zeolite by Crystallization of Silanized Protozeolitic Units. Catalysis Today 345: 27-38.

31. Bauer F, Meyer R, Bertmer M, Naumov S, Al-Naji M, et al. (2021) Silanization of Siliceous Materials, Part 3: Modification of Surface Energy and Acid-base Properties of Silica Nanoparticles Determined by Inverse Gas Chromatography (IGC). Colloids and Surfaces A: Physicochemical and Engineering Aspects 618: 1-12.

32. Song W, Justice R E, Jones C A, Grassian V H, Larsen S C, et al. (2004) Synthesis, Characterization, and Adsorption Properties of Nanocrystalline ZSM-5. Langmuir 20(19): 8301-8306.

33. Yang R, He R D (1994) Studies on HZSM-5 Zeolites Modified with Silanes. Journal of Fuel Chemistry and Technology 22: 393-399.

34. Zhang S, Li M, Li W, Li YW, Liu F, et al. (2021) Comparison and Analysis of Toluene Adsorption Properties of ZSM-5 Molecular Sieve Treated by Different Modification Methods: Adsorption Kinetic and Mechanism Studies. China Petroleum Processing and Petrochemical Technology 23(1): 76-87.

35. Kurzydym I, Czekaj I (2022) The effect of the presence of a hydroxyl group on the vibration frequencies of NO and NH3 adsorbates on Cu-Zn bimetallic nanoparticles in ZSM-5 and FAU zeolite – a DFT study. J Molecular Structure 1255: 132440.

36. Sivasankar N, Vasudevan S (2004) Temperature-Programmed Desorption and Infrared Spectroscopic Studies of Benzene Adsorption in Zeolite ZSM-5. J Phys Chem B 108(31): 11585-11590.

37. Wang KY, Wang X S, Li G, Long HY (2022) Characterization and Catalytic Activity of Silylated Nanoscale ZSM-5. CHINESE JOURNAL OF CATALYSIS 41: 2504-2510.

38. Miyamoto M, Ono S, Oumi Y, Uemiya S, Van der Perre S, et al. (2019) Nanoporous ZSM 5 Crystals Coated with Silicalite 1 for Enhanced p Xylene Separation. ACS Appl Nano Mater 2(5): 2642-2650.

39. Zhang M J, Qian WX, Ma HF, Ying WY, Zhang HT, et al. (2024) Molecular Insights into Adsorption and Diffusion Properties of CO2/CH4 in Cation-Exchanged ZSM 5 Zeolites. J Phys Chem C 128(1): 6962-6970.

40. Zhang Y W, Yu J Y, Yeh Y H, Gorte R J, Rangarajan S, et al. (2015) An Adsorption Study of CH4 on ZSM-5, MOR, and ZSM-12 Zeolites. J Phys Chem C 119: 28970-28978.

41. Zhao H, Ma J H, Zhang Q Q, Liu Z P, Li R F, et al. (2014) Adsorption and Diffusion of n Heptane and Toluene over Mesoporous ZSM 5 Zeolites. Ind Eng Chem Res 53: 13810-13819.

42. Khatrin I, Kusuma RH, Kadja GTM, Krisnandi YK (2023) Significance of ZSM-5 Hierarchical Structure on Catalytic Cracking: Intra- vs Inter-crystalline Mesoporosity. Inorganic Chemistry Communications 149: 110447.

43. Yu M, Noble R D, Falconer J L (2011) Zeolite Membranes: Microstructure Characterization and Permeation Mechanisms. Accounts of Chemical Research 44(11): 1196-1206.

44. Li H Z, Dong L X, Zhao L, Cao L Y, Gao J, et al. (2017) Enhanced Adsorption Desulfurization Performance over Mesoporous ZSM 5 by Alkali Treatment. Ind Eng Chem Res 56: 3813-3821.

45. Liu Q, He P P, Qian X C, Fei Z Y, Zhang Z X, et al. (2017) Enhanced CO2 Adsorption Performance on Hierarchical Porous ZSM 5 Zeolite. Energy Fuels 31(12): 13933-13941.

46. Yeh Y H, Gorte R J, Rangarajan S, Mavrikakis M (2016) Adsorption of Small Alkanes on ZSM 5 Zeolites: Influence of Brønsted Sites. J Phys Chem C 120: 12132-12138.

47. Maag A R, Tompsett G A, Tam J (2019) ZSM-5 Decrystallization and Dealumination in Hot Liquid Water. Physical Chemistry Chemical Physics 21(32): 17880-17892.

48. Wichterlovfi B, Cejka J (1992) A Comparison of the Ethylation of Ethylbenzene and Toluene on Acid, Cationic and Silylated ZSM-5 Zeolites. Catalysis Letters 16: 421-429.

49. Kang M L, Nam S K, Muhammad N, Jeong-Chul K, Hae S C, et al. (2021) Postsynthetic Modification of Zeolite Internal Surface for Sustainable Capture of Volatile Organic Compounds under Humid Conditions. ACS Appl Mater Interfaces 13(45): 53925-53934.

50. Li C.L, Liu CL, Yang HJ, Ben XY, Lv TY, et al. (2013) Study on Hydrophobic Silylation Modification of High Silica Molecular Sieve ZSM-5. Chemical Research and Application 25: 236-239.

51. Wang J, Wu Z, Niu Q (2021) Highly Efficient Adsorptive Removal of Toluene Using Silicon-Modified Activated Carbon with Improved Fire Resistance. Journal of Hazardous Materials 415: 125753-125753.

52. Xu L, Okrut A, Rea T, Chaudhuri K, Han JY, et al. (2023) Control of Zeta Potential of Hierarchical Mesoporous Zeolite Y via Inorganic Surface Modification without Micropore Blockage and Phase Separation. Cryst. Growth Des 23: 5601-5613.

53. Wang Y, He T, Cao J, Li K, Wang C, et al. (2025) Waste-to-microporous framework: Al/Si fractionation of coal fly ash coupled with waste PET conversion for separated synthesis of high-porosity MIL-53(Al) and ZSM-5 toward efficient dyes and CO2 capture. J Molecular Structure 1335: 141984.

ISSN: 2574-1241

DOI: 10.26717/BJSTR.2025.63.009837

Yulong Zhang and Jiali Zhang. Biomed J Sci & Tech Res